Available online at www.sciencedirect.com
ScienceDirect
Ceramics International 35 (2009) 771–778
CERAMICS INTERNATIONAL
www.elsevier.com/locate/ceramint

Microstructure and mechanical properties of hot-pressed B_4C/TiC/Mo ceramic composites

Deng Jianxin *, Sun Junlong

Department of Mechanical Engineering, Shandong University, Jinan 250061, Shandong Province, PR China

Received 3 September 2007; received in revised form 12 December 2007; accepted 19 February 2008
Available online 28 June 2008

Abstract

Boron carbide (B_4C)/TiC/Mo ceramic composites with different content of TiC were produced by hot pressing. The effect of TiC content on the microstructure and mechanical properties of the composites has been studied. Results showed that chemical reaction took place for this system during hot pressing sintering, and resulted in a B_4C/TiB_2/Mo composite with high density and improved mechanical properties compared to monolithic B_4C ceramic. Densification rates of the B_4C/TiC/Mo composites were found to be affected by additions of TiC. Increasing TiC content led to increase in the densification rates of the composites. The sintering temperature was lowered from 2150 °C for monolithic B_4C to 1950 °C for the B_4C/TiC/Mo composites. The fracture toughness, flexural strength, and hardness of the composites increased with increasing TiC content up to 10 wt.%. The maximum values of fracture toughness, flexural strength, and hardness are 4.3 MPa $m^{1/2}$, 695 MPa, and 25.0 GPa, respectively.

Keywords: B. Composites; C. Mechanical properties; D. Borides; D. Carbides

1. Introduction

Boron carbide (B_4C) has high hardness, high wear resistance, high melting point, good chemical inertness, high thermal conductivity as well as high cross-section for neutron absorption [1], that make it promising candidate for wear resistance component. B_4C is best recognized for its hardness and abrasion resistance. After diamond and cubic boron nitride, B_4C is the third hardest of the technically useful materials. Sand blasting nozzles made of dense sintered B_4C are extremely wear-resistance. Under highly abrasive conditions B_4C outperforms other hard materials [2–4]. Moreover the low density of B_4C and its high Young's modulus recommend this material for the construction of light-weight armour, as is need in the military helicopter and similar aero-applications [5].

Compared with the ceramics such as Si_3N_4, SiC, ZrO_2, etc., the strength and fracture toughness of monolithic B_4C ceramic material are rather low (about 200–400 MPa), and its fracture toughness is about 2–3 MPa $m^{1/2}$ [1]. Moreover, the poor sinterability of B_4C limits its application because both high temperature and high pressure are required for a complete densification [6,7]. In earlier studies [8–15], some of the B_4C-based-composites, e.g., B_4C/(W,Ti)C, B_4C/SiC, B_4C/TiB_2, B_4C–CrB_2, $B_4C/TiB_2/MB_2$, B_4C/MB_2, B_4C/Al, have been developed and used in various applications, mechanical properties and microstructure studies on them are also extensively carried out. It has been shown that the additions of secondary phases to B_4C matrix can improve its mechanical properties, i.e., fracture toughness and flexural strength.

In this paper, B_4C-based ceramic composites with different content of TiC were produced by hot pressing. The mechanical properties and the microstructure of these composites have been studied. Particular attention was paid to the effect of TiC additions on the mechanical properties and microstructure.

2. Experimental procedure

2.1. Materials and processing

The starting powders used to fabricate the B_4C/TiC/Mo composites are listed in Table 1 with their particle size, purity and manufacturer. B_4C/Mo (mass ratio 18:1) was used as the base material. Additions of TiC particles were added to B_4C/Mo matrix according to the combinations listed in Table 2. The

* Corresponding author. Tel.: +86 531 88392047.
E-mail address: jxdeng@sdu.edu.cn (D. Jianxin).

0272-8842/$34.00
doi:10.1016/j.ceramint.2008.02.014

Table 1
Particle size, purity and manufacturer of the starting powders

Starting powder	Average particle size (μm)	Purity (%)	Manufacture
B_4C	3–5	>95	Mudanjiang Abrasive Works, PR China
TiC	1–2	>99	Zhuzhou Cemented Carbide Works, PR China
Mo	1–3	>99	Zhuzhou Cemented Carbide Works, PR China

Table 2
Compositions, sintering parameters, and relative densities of the composites

Sample	Compositions (wt.%)			Sintering parameter		Relative density (%)	Grain size (μm)
	B_4C	TiC	Mo	Temperature (°C)	Time (min)		
B00	100	0	0	2150	65	95.0	5–8
BTM0	94.7	0	5.3	1950	50	96.5	1–2
BTM05	90.0	5	5	1950	50	99.1	1–2
BTM10	85.3	10	4.7	1950	50	99.2	1–2
BTM15	80.5	15	4.5	1950	50	99.0	1–2
BTM20	76	20	4	1950	50	98.5	1–2

combined powders were prepared by wet ball milling in alcohol for 100 h with cemented carbide balls. The container with internal diameter 150 mm is made of cemented carbide, and is rotated with a speed of 100 rpm. The average diameter of the carbide ball is 6 mm. The average particle size of the milled combined powders is less than 1.5 μm. Following drying, the final densification of the compacted powder was accomplished by hot pressing with a pressure of 35 MPa in argon atmosphere for 10–65 min to produce a ceramic disk. The maximum temperature employed for hot pressing was 2150 °C.

2.2. Material characterization

Densities of the hot-pressed disks were measured by the Archimedes's method. Test pieces of 3 mm × 4 mm × 36 mm were prepared from the disk by cutting and grinding using a diamond wheel and were offered for measurement of flexural strength, Vickers hardness and fracture toughness. Three-point-bending mode was used to measure the flexural strength over a 30 mm span at a crosshead speed of 0.5 mm/min. Fracture toughness measurement was performed using indentation method in a hardness tester (MH-6) using the formula proposed by Cook and Lawn [16]. On the same apparatus the Vickers hardness was measured on polished surface with a load of 98 N. Data for hardness, flexural strength, and fracture toughness were gathered on five specimens.

XRD (*D*/max-2400) analysis was undertaken to identify the crystal phases present after sintering. The microstructures of sintered materials were studied on fracture surfaces and polished section by scanning electron microscopy (HITACHI S-570).

3. Results and discussion

3.1. X-ray diffraction phase analysis

Fig. 1 shows the X-ray diffraction analysis of the BTM10 composite after hot pressing at temperature 1950 °C for 50 min. It is obvious from Fig. 1 that TiB_2 is newly formed phases, and are resulted from the reaction of B_4C with TiC. No trace of TiC was found in the sintered materials when these phases had been added in the powder compacts prior to sintering, showing that a complete reaction occurred during sintering. The reaction formulas are as follows [8]:

$$B_4C + 2TiC \rightarrow 2TiB_2 + 3C \quad (1)$$

According to the thermo-chemical data for the B_4C–TiC system, the ΔG_T^θ (Gibbs free energy) of above reaction at 2100 K can be calculated. The value of ΔG_T^θ is −201.800 kJ/mol [17]. It is negative. Therefore, the above chemical reaction is proved to occur.

3.2. Densification of the composites

Densification rates of the B_4C-based ceramic composites were found to be affected by additions of TiC. Increasing content of TiC led to increase the densification rates of composites as can be seen in Fig. 2 and Table 2. The relative

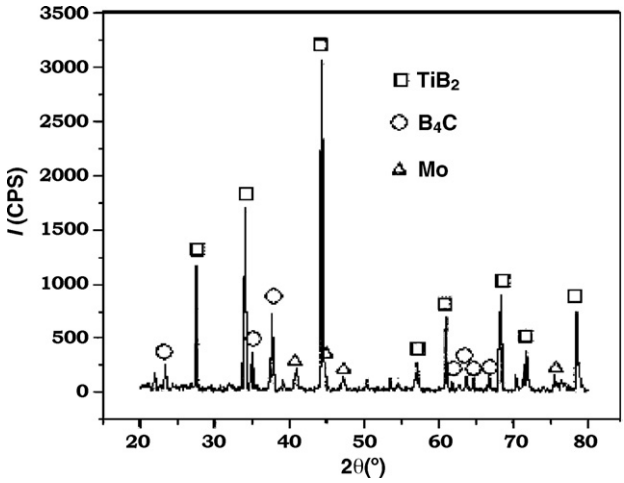

Fig. 1. X-ray diffraction analysis of the BTM10 composite after hot pressing at temperature of 1950 °C for 50 min.

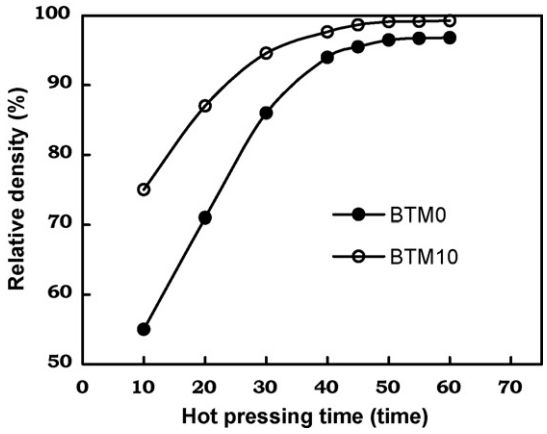

Fig. 2. Densification behaviors of BTM0 and BTM10 composites (hot pressing temperature: 1950 °C).

density of BTM10 composite reaches 99.2% after hot pressing at temperature of 1950 °C for 50 min; while it is only 95.0% for monolithic B_4C ceramic after hot pressing at temperature of 2150 °C for 65 min. The hot pressing temperature was lowered from 2150 °C for monolithic B_4C to 1950 °C for B_4C/TiC/Mo composites.

3.3. Mechanical properties

Fig. 3 shows the effect of TiC additions on the mechanical properties of the B_4C/TiC/Mo composites. It was found that the flexural strength increased with increasing of TiC content up to 10 wt.%, and rose from 540 MPa for BTM0 to 695 MPa for BTM10 composite, representing a maximum strengthening increase of 155 MPa. Within further increasing the TiC content, the flexural strength decreased with increasing TiC content. The trend of the fracture toughness and hardness are the same as that of the flexural strength. The maximum values of fracture toughness and hardness are 4.3 MPa $m^{1/2}$ and 25.0 GPa, respectively for BTM10 composite.

The effect of sintering time and hot pressing temperature on the mechanical properties of BTM10 composite are shown in Figs. 4 and 5, respectively. For a sintering time of less than 45 min, the flexural strength, fracture toughness, and hardness of the BTM10 composite increase with sintering time, and within a further increase, they almost remain constant. On the other hand, when the hot pressing temperature is lower than 1950 °C, the flexural strength, fracture toughness, and hardness continuously increase with the hot pressing temperature, and within a further increase, they shows no much changes.

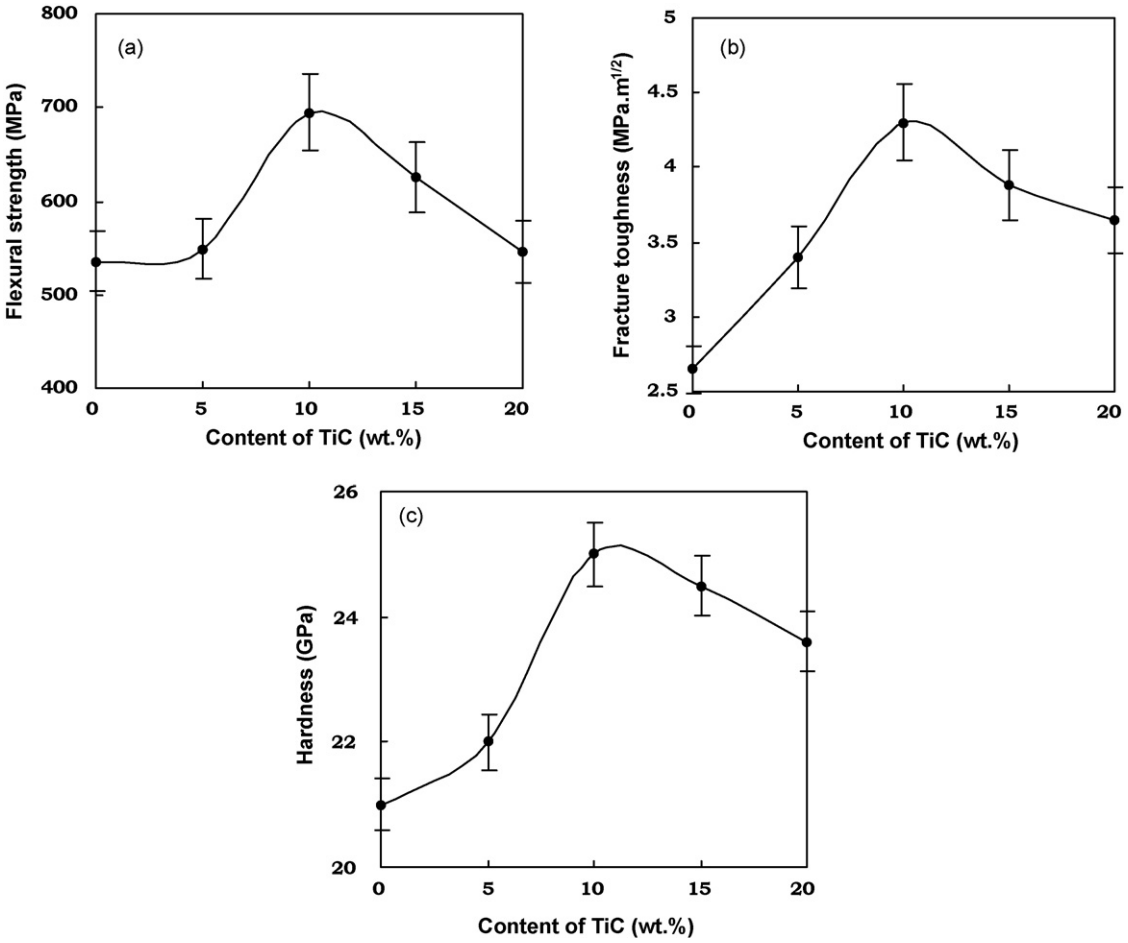

Fig. 3. Effect of TiC additions on the mechanical properties of the B_4C/TiC/Mo composites (hot pressing temperature: 1950 °C, sintering time: 50 min).

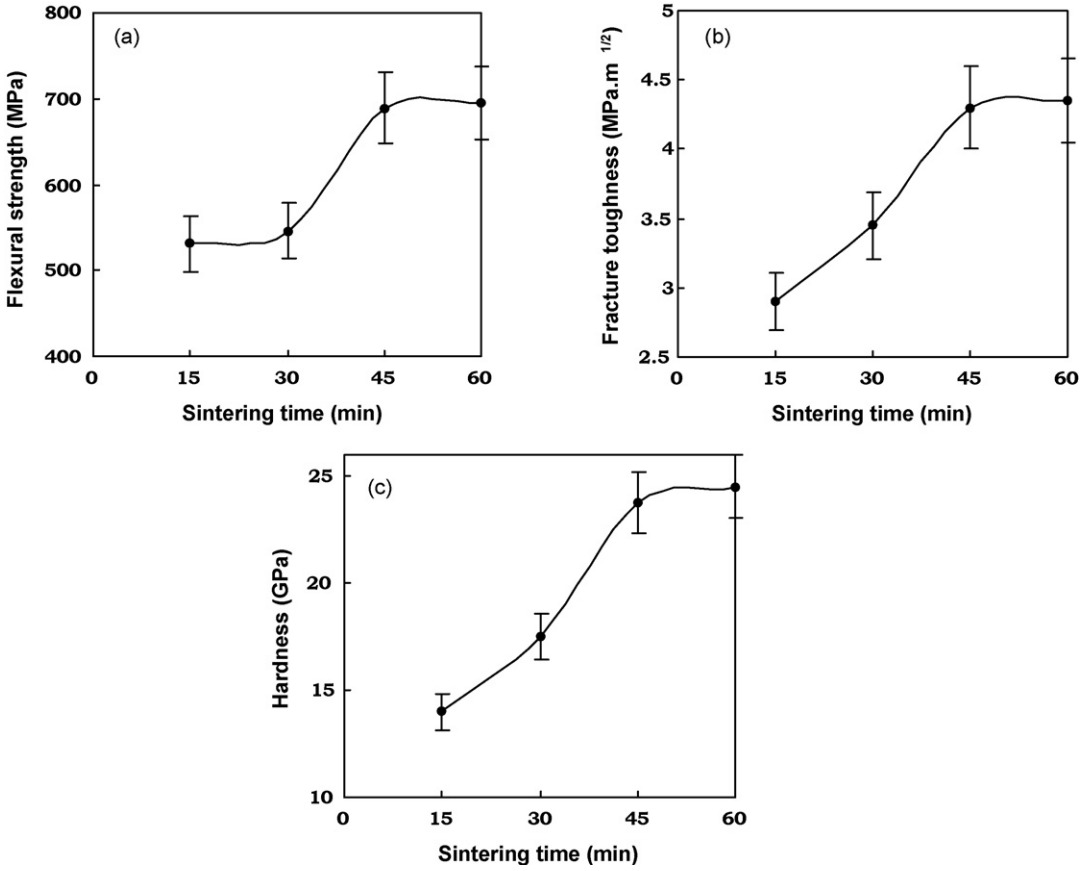

Fig. 4. Effect of sintering time on the mechanical properties of BTM10 composite (hot pressing temperature: 1950 °C).

3.4. Microstructural characterization

Fig. 6 shows the SEM micrographs of the fracture surfaces of monolithic B_4C (B00) after hot pressing at temperature of 2150 °C for 65 min. It is shown that the monolithic B_4C exhibited a flat fracture surface, resulting from the transgraular fracture mode, and there are a lot of obvious pores located at the B_4C grain boundary. These pores may serve as fracture origins and cause the degradation of strength and fracture toughness. A remarkable increase of the grain size (5–8 μm) was also observed (see Fig. 6b).

Fig. 7 shows the SEM micrographs of the fracture surface of BTM10 composite after hot pressing at temperature of 1800 and 1950 °C. From these SEM micrographs, different morphologies of the composites can be seen clearly. It is not a dense body, and reveals quite a number of cavities at the fracture surface when sintered at 1800 °C (see Fig. 7a). While the composite sintered at 1950 °C is dense, porosity is virtually absent, and shows an intergranular fracture mode (see Fig. 7b). The grain sizes ranged from 1 to 2 μm. The addition of TiC phase seems to have inhibited the grain growth of the composite.

Fig. 8 shows typical microstructure from the polished surface of hot-pressed monolithic B_4C. It is shown that there are quite a number of cavities on the polished surface of monolithic B_4C.

Typical microstructures from the polished surface of BTM10 composite after hot pressing at temperature of 1850 and 1950 °C are shown in Fig. 9. The gray areas as identified by EDX analysis are B_4C and the white areas are of TiB_2. It is noted that the TiB_2 particles seem quite uniformly distributed throughout the microstructure when sintered at 1950 °C (see Fig. 9b); while it shows a loose structure on the polished surface when sintered at 1850 °C (see Fig. 9a).

4. Discussion

For particle composites, several toughening mechanisms have been proposed [18–21]. Crack pinning, crack deflections, microcracking, crack bridging, and residual stresses. A number of these mechanisms can be active at the same time, making it difficult to indicate a prevailing phenomenon. In the present case, since the thermal expansion coefficients of the constituent phases are quite difference (see Table 3), the fracture toughness increase can be attributed more probably to the mechanisms such as residual stresses and crack deflection.

The compressive thermal residual stress in the matrix is generated when the coefficients of the thermal expansion (CTE) of the particle exceeds that of the matrix. Since the existence of this thermal residual stress in the particle reinforced ceramic composite, the fracture toughness K_{IC} of the material is

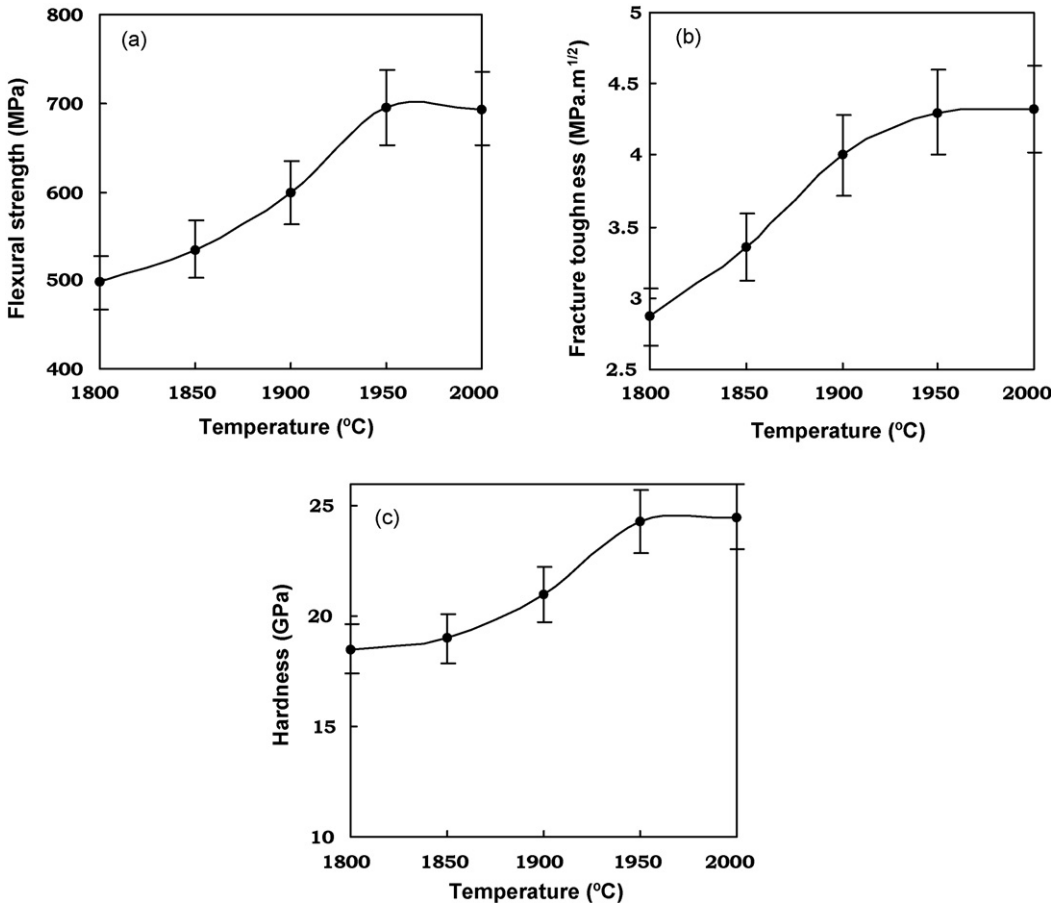

Fig. 5. Effect of hot pressing temperature on the mechanical properties of BTM10 composite (sintering time: 50 min).

expressed as [19–21]:

$$K_{IC} = K_{I0} + 2q\sqrt{\frac{2D}{\pi}} \quad (2)$$

where K_{I0} is the critical stress intensity factor of the matrix, q is the local thermal residual compressive stress, D is the length of the compressive stress zone which in this case is the average particulate spacing. If the dispersed phase of the same grain size is distributed uniformly in the matrix, then $D = \lambda - d$, where the average distance between the particles of the dispersed phase is λ.

The existence of the local stress q decreases the stress intensity factor, ΔK_I. From Eq. (2) this decrease is

$$\Delta K_I = K_{IC} - K_{I0} = 2q\sqrt{\frac{2(\lambda - d)}{\pi}} \quad (3)$$

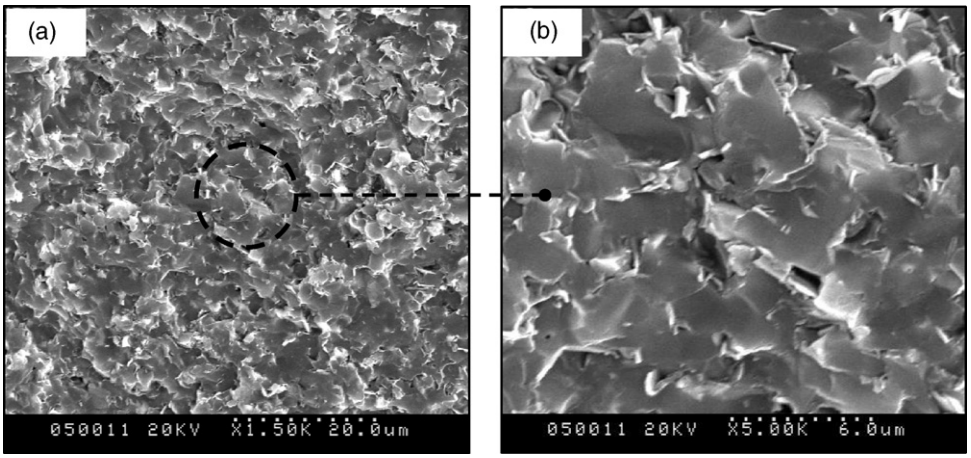

Fig. 6. SEM micrographs of the fracture surfaces of (a) monolithic B_4C after hot pressing at temperature of 2150 °C for 65 min and (b) enlarged SEM micrograph corresponding to (a).

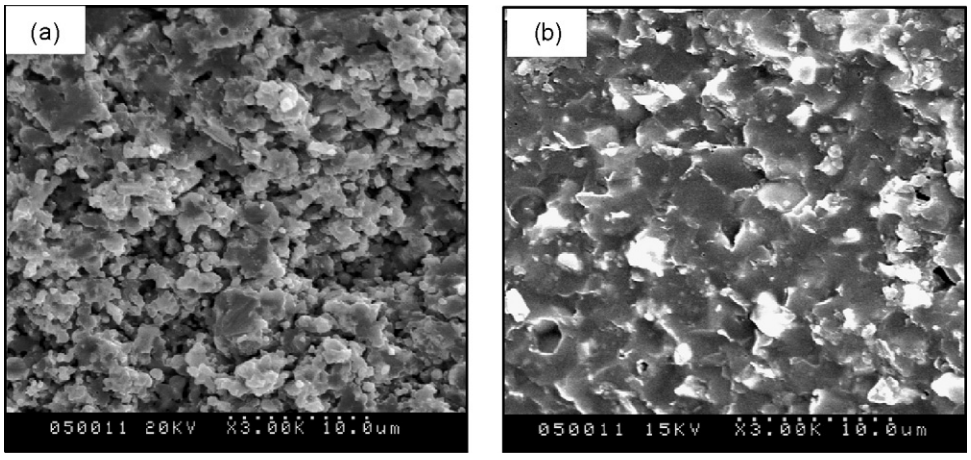

Fig. 7. SEM micrographs of the fracture surfaces of BTM10 composite after hot pressing at temperature of (a) 1800 °C and (b) 1950 °C.

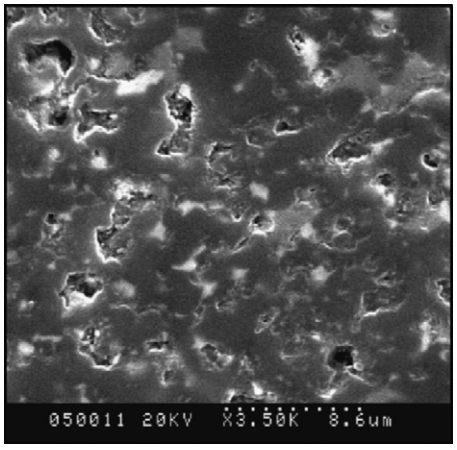

Fig. 8. SEM micrograph of the polished surface monolithic B_4C after hot pressing at temperature of 2150 °C for 65 min.

where [20]

$$\lambda = \frac{1.085d}{\sqrt{V_p}} \tag{4}$$

$$q = \frac{2E_m V_p \beta \Delta\alpha \Delta T}{A} \tag{5}$$

$$A = (1 - V_p)(\beta + 2)(1 + \nu_m) + 3\beta V_p(1 - \nu_m) \tag{6}$$

$$\beta = \frac{(1 + \nu_m)E_p}{(1 - 2\nu_p)E_m} \tag{7}$$

where E and ν express the elastic modulus and the Poisson's ratio, respectively, while the subscript p and m indicates the dispersed phase and the matrix, respectively. V_p means the volume fraction of the dispersed phase, $\Delta\alpha$ indicates the

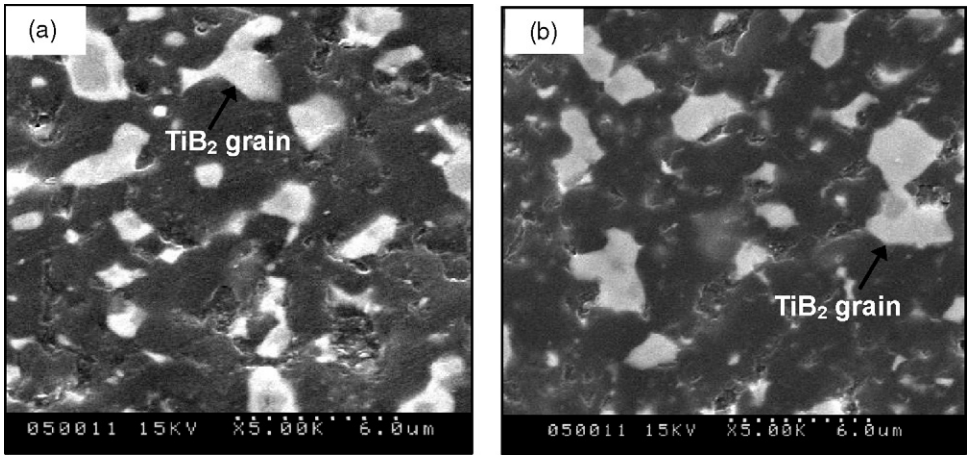

Fig. 9. Typical microstructures of the polished surface of BTM10 composite after hot pressing at temperature of (a) 1850 °C and (b) 1950 °C.

Table 3
Properties of B_4C, TiB_2 and Mo [1,5]

	Density (g/cm^3)	Melting point (°C)	Hardness (GPa)	Elastic modulus (GPa)	Poisson's ratio	Thermal expansion coefficient (10^{-6} K^{-1})
B_4C	2.52	2450	29–46	445	0.25	4.5–5.5
TiB_2	4.52	2790	25–33	529	0.28	8.1

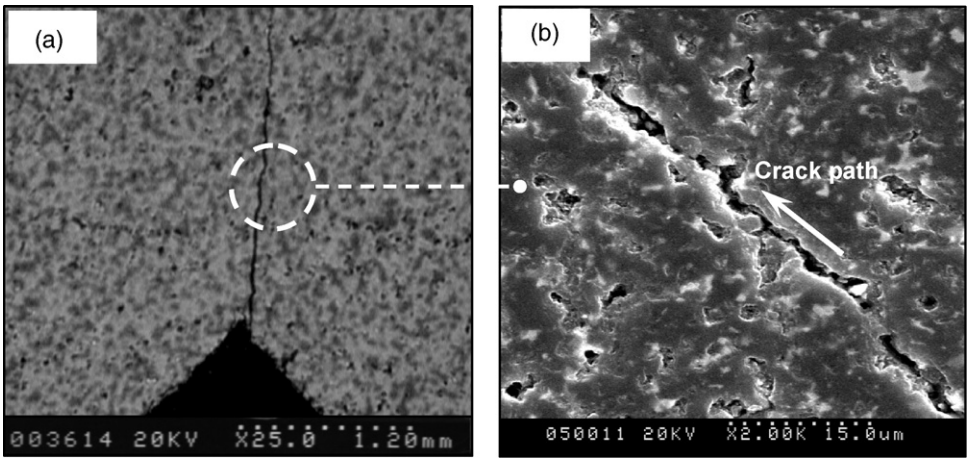

Fig. 10. Crack path produced by Vickers indentation on the polished surface of monolithic B_4C.

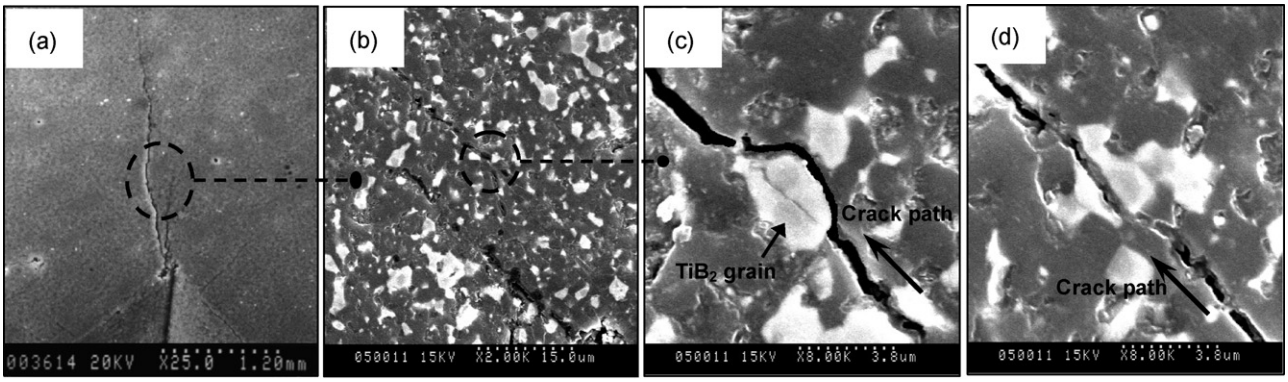

Fig. 11. Crack path produced by Vickers indentation on the polished surface of BTM10 composite.

difference in the thermal expansion between the particle and the matrix, ΔT is the temperature change.

According to the above theoretical analyses, corresponding calculations are carried out with an example of B_4C/10 vol.% TiB_2 composite where B_4C is the matrix and TiB_2 acts as the dispersed phase owing to the reaction of B_4C with TiC in present study. With the data of the material properties shown in Table 3, the result is as follows:

$$\Delta K_I = -0.793\ \text{MPa}\,\text{m}^{1/2} \tag{8}$$

$\Delta K_I < 0$ means the stress intensity factor is decreased by ΔK_I as a result of the action of the thermal residual stress. However, the decrease in the stress intensity factor by ΔK_I is equivalent to the increase in the crack growth resistance by the same amount ΔK_I. Therefore, the corresponding toughening increment of B_4C/10 vol.% TiB_2 composite owing to compressive thermal residual stress is 0.792 MPa $m^{1/2}$.

An additional mechanism which contributes to the toughening of particle-reinforced ceramic composite is crack deflections [18,19]. Fig. 10 shows the path of a crack produced by Vickers indentation on the polished surface of hot-pressed monolithic B_4C. It is noted that crack deflection rarely occurred (see Fig. 10b). The path of a crack produced by Vickers indentation on the polished surface of BTM10 composite is shown in Fig. 11. It is shown that by incorporating TiC into B_4C, the cracks suffered a larger deflection (see Fig. 11b and c) and bridging effect (see Fig. 11d) during the course of the propagation. This made the newly ruptured surface areas become larger, and a greater amount of rupture energy was consumed. The crack deflection was thought to be caused by the residual stress generated by the difference in the thermal expansion coefficient between B_4C and TiB_2 in the composites [8]. Thus, the improvement of fracture toughness may be also attributed to the crack deflection mechanism triggered by internal stresses due to the thermal expansion coefficient mismatch of B_4C matrix and TiB_2 dispersed phases.

The flexural strength of the composite is greatly improved with respect to B_4C matrix when the composite are nearly fully dense and with finer microstructure (see Table 2). So strong grain refinement, higher relative density, more uniform microstructure associated with the reduction of porosity may be the direct consequence of the higher strength of the composites.

5. Conclusions

B_4C/TiC/Mo ceramic composites with different content of TiC were produced by hot pressing. Particular attention was

paid to the effect of TiC additions on the mechanical properties and microstructure. The following conclusions were obtained:

1. Chemical reaction took place for this ceramic system during hot pressing, and resulted in a B_4C/TiB_2/Mo composite with high density and improved mechanical properties compared to monolithic B_4C ceramic.
2. Densification rates of the composites were found to be affected by additions of TiC. Increasing content of TiC led to increase the densification rates of the composites. The hot pressing temperature was lowered from 2150 °C for monolithic B_4C to 1950 °C for B_4C/TiC/Mo composites.
3. The fracture toughness, flexural strength, and hardness of the composites increased with increasing of TiC content up to 10 wt.%. The maximum values of fracture toughness, flexural strength, and hardness are 4.3 MPa $m^{1/2}$, 695 MPa, and 25.0 GPa, respectively.

Acknowledgements

This work was supported by "the National Natural Science Foundation of China (50675120)", "the Key Science and Technology Project of Shandong Province (2006GG2204017)".

References

[1] F. Thevenot, Boron carbide—a comprehensive review, Journal of the European Ceramic Society 6 (1990) 205–225.
[2] Deng Jianxin, Erosion wear of boron carbide nozzles by abrasive air-jets, Materials Science Engineering A 408 (1–2) (2005) 227–233.
[3] K.A. Schwetz, L.S. Sigl, J. Greim, Wear of boron carbide ceramics by abrasive waterjets, Wear 181–183 (1995) 348–355.
[4] Deng Jianxin, Sun Junlong, Sand erosion performance of B_4C based ceramic nozzles, International Journal of Refractory Metals & Hard Materials 26 (3) (2008) 128–134.
[5] Heinrich Knoch, Non-oxide technical ceramics, in: 2nd European Symposium on Engineering Ceramics, Elsevier Applied Science, (1987), pp. 151–169.
[6] S.L. Dole, S. Prochazka, Robert H. Doremus, Microstructural coarsening during sintering of boron carbide, Journal of American Ceramic Society 72 (6) (1989) 958–966.
[7] S.L. Dole, S. Prochazka, Densification and microstructure in boron carbide, Ceramic Engineering Science Proceedings 16 (1985) 1151–1160.
[8] Deng Jianxin, Zhou Jun, Feng Yihua, Ding Zeliang, Microstructure and mechanical properties of hot-pressed B_4C/(W,Ti)C ceramic composites, Ceramics International 28 (4) (2002) 425–430.
[9] Z. Panek, The synthesis of SiC/B_4C ceramics by combustion during hot pressing, Journal of the European Ceramic Society 11 (1993) 231–236.
[10] L.S. Sigl, Microcracking in B_4C/TiB_2 composites, Journal of American Ceramic Society 78 (9) (1995) 2374–2380.
[11] T. Grazian, A. Bellosi, Production and characteristics of B_4C/TiB_2 composites, Key Engineering Materials 104–107 (1995) 125–132.
[12] Suzuya Yamada, Kiyoshi Hirao, Yukihiko Yamauchi, Shuzo Kanzaki, B_4C–CrB_2 composites with improved mechanical properties, Journal of the European Ceramic Society 23 (2003) 561–565.
[13] R. Telle, G. Petzow, Strengthening and toughening of boride and carbide hard material composites, Material Science and Engineering A 105/106 (1988) 97–104.
[14] L.S. Sigl, Processing and mechanical properties of boron carbide sintered with TiC, Journal of the European Ceramic Society 18 (1998) 1521–1529.
[15] A.K. Bhattacharya, J.J. Petrovic, Ductile phase toughening and R-curve behavior in a B_4C–Al cermets, Journal of Material Science 27 (1992) 2205–2210.
[16] R.F. Cook, B.R. Lawn, A modified indentation toughness technique, Journal of American Ceramic Society 66 (11) (1983) C-200–C-201.
[17] Sun Junlong, Development of new B_4C composite ceramic nozzle and study on its erosion mechanisms, Ph.D. Dissertation, Shandong University, 2007.
[18] A.G. Evans, Perspective on the development of high toughness ceramics, Journal of American Ceramic Society 73 (2) (1990) 187–195.
[19] R.W. Steinbrech, Toughening mechanisms for ceramic materials, Journal of the European Ceramic Society 10 (1992) 131–142.
[20] Minoru Taya, S. Hayashi, Albert S. Kobayashi, Toughening of a particulate-reinforced ceramic matrix composite by thermal residual stress, Journal of American Ceramic Society 75 (5) (1990) 1382–1391.
[21] Borwen Lin, Takayoshi Iseki, Effect of thermal residual stress on mechanical properties of SiC/TiC composites, British Ceramic Transactions 91 (1992) 1–5.